

Development and Investigation of a Textile Heating Element Ensuring Thermal Physiological Comfort

DOI: 10.5604/01.3001.0014.2385

SRI Center for Physical Sciences
and Technology (FTMC),
Savanorių pr. 231,
LT-02300 Vilnius, Lithuania,
* e-mail: ingrida.padleckiene@ftmc.lt

Abstract

The aim of this research was to develop a flexible heating element and investigate its heating capability in simulated wearing conditions. Polyester silver (Ag)-plated yarns incorporated in the reverse side of the knitted structure were used to provide electrical conductivity. A special knitted structure was selected to keep conductive yarn only in the reverse side of the material. All the heating element was made using only textile materials and yarns. A temperature sensor thermistor was used as an electronic element to follow the body temperature, and the remaining elements ensuring a correct electric circuit and heating were made of textile. Another type of heating element was produced using enamelled copper wire, which was inserted into the knitted fabric structure. Investigation of both types of heating elements was made by determining the dependences of the heating elements' temperatures on the current and voltage applied. It was concluded that the heating element with silver plated yarns used gave out warmth more evenly over all the resistive area. The microcontroller, which has a heating dynamics data storage function, was programmed to control the operations of the two heating elements. A model of an intelligent apparel product with two heating elements ensuring a comfortable microclimate for the user was created. Field tests were performed for the model created by wearing the product and setting the temperatures of both heating elements, for which the continuous operating time was determined.

Key words: e-textile, wearable electronics, heating element, thermal physiological comfort.

Introduction

In the last few years, there has been growing interest in and a big demand for everyday electronical textiles which are physically flexible, comfortable, breathable, lightweight, durable, and with various wearable technologies integrated. The e-textile market is growing fast, and the latest technologies are applied to smart textiles.

Intelligent heating textile can play an important role in the protection and safety of humans. It can be used in protective wear in outdoor or low-temperature environments. Such apparel is able to control the body temperature and prolong comfortable conditions. As well, heating textile can be used in intelligent sportswear for heating the muscles and keeping them warm, ready for the best performance. Various additional applications are possible, such as heated bed linings, footwear, and furniture, among others. Further textile actuators like heating fabrics have been used in numerous and varied fields, such as sports, leisure, medical and automotive [1-3].

Extensive research is being done worldwide to develop fabrics that provide comfort to the wearer, while offering active protection against a cold environment. Very smart heating textiles should have

three main features: ensuring freedom of movement, communication with the human body temperature, and actively keeping the body temperature stable. Various textile manufacturing technologies and treatments such as knitting, weaving, non-woven, spinning, breading, coating/laminating, printing, sewing, embroidery and chemical treatment could be used for integrating a heating element into textile material [4-7].

The main criteria for the selection of yarns for the manufacture of a knitted resistive heating element are as follows: low electrical resistance of yarns; temperature evenness of the element for a long time, and the suitability of the yarns for knitting [8]. The next consideration is whether the material is suitable for clothing. The basic pre-requisites for a heating element to be applied to clothing are softness, flexibility and wash ability [9]. The integration of electronic products into fabric products is very difficult because of their manufacturing processes [10, 11] and physical properties, which differ greatly: fabric is flexible, and most electronic components are solid. Although smart textiles are progressing very rapidly [12, 13], connectivity, materials, fabrication and wear are still challenges for smart textiles [14].

Smart clothing is made with conductive yarns where an electrical current is re-

quired to pass through the fabric [15]. Heating properties can be achieved by using conductive materials. Temperature control is one of the most important functions of clothes. All the heating materials currently available in the market need high wattage power supplies. Therefore, there is a need for such heating elements that can operate at low voltages [16].

Scientists presented research where they investigated knitted heating fabrics that were designed and fabricated using silver-plated compound yarns and polyester staple fibre spun yarns. Thermo-electric properties were investigated by performing a series of experiments in which the ageing time and temperature were increased. Knitted heating fabrics have wide application prospects in the active warming field because of the many advantages, such as an even surface temperature field in the heating process, structure simplicity, flexibility, etc. [17]. Investigation [18] concluded that polypyrrole heating fabric is suitable for next-to-body heating applications, which can be engineered by controlling the optimum electrical pathways provided by the network of polypyrrole molecular chains, together with correct power supply levels, to work under a defined fabric strain range. The purpose of the current research was to obtain a new material that could help to develop heating fabrics with improved textile properties.

The results obtained [19] demonstrate that the PU@CB@FAB system is a promising candidate for low cost wearable, flexible, and stretchable heaters. This system can be further developed for heating applications by using different additives such as IR reflectors. In addition, the system constructed can be developed as super capacitors for application in wearable electronics. This article introduces a new type of flexible, lightweight and comfortable-to-the-wearer heating element for an intelligent textile product.

Materials and methods of the investigation

Two different knitted heating elements were designed and investigated in this research.

For the manufacturing of electro-conductive knitted heating element I, a 10E gauge flat double needle-bed knitting machine SES 122-S (Shima Seiki, Japan) was used. Heating element I was produced on the basis of weft-knitted fabric of combined pattern from merino wool/polyamide, polyester spun yarns and enamelled copper wire with a diameter of 0.07 mm. This continuous wire was inserted into the structure of knitted fabrics in different lengths and distances. A tech-

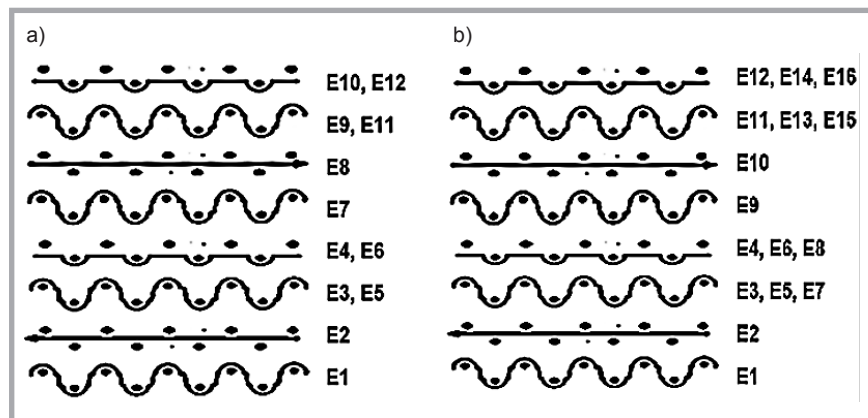


Figure 1. Pattern of the weft knitted fabric structure used for heating element I: a) heating element I-1, b) heating elements I-2 and I-3

nical description of the 3 heating elements used, with different arrangements of electroconductive wire, is given in Table 1. The combined pattern and schematic illustration of the knitted structures are presented in Figure 1 and Figure 2. Resistivity depends on the length of the enamelled copper wire the longer the copper wire, the higher the resistivity.

For manufacturing electro-conductive knitted heating element II, a 20E gauge FIHN (“Orizio”, Italy) circular knitting machine was used. A detailed description of the finished three-thread fleecy knitted fabric is given in Table 2, and the knitted

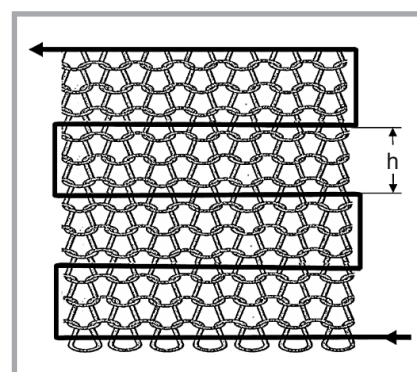


Figure 2. Schematic illustration of the weft knitted fabric structure used for heating element I: h – distance between enamelled wires in the fabric.

Table 1. Description of weft knitted fabric used for heating element I. Note: Number of stitches of all knitted structures per unit length and unit area: courses, P_V (front/back side) – 12/6 cm^{-1} ; wales, P_H – 4 cm^{-1} .

Code of heating element I	Type of yarn, linear density/diameter, tex/mm	Arrangement of yarns and conductive wire in pattern courses (knitting feeds) (Figure 4)	Heating area (length x height), cm
I-1	Merino Wool/PA (70/30%) spun yarns, 36.0 x 2 + PET spun yarns with bio-ceramic additives Mirawave® 29.4 Enamelled copper wire, 0.07 mm (length 10 m, distance between wires in the fabric 0.5 cm)	E1, E3, E4, E5, E6, E7, E9, E10, E11, E12 E2, E8	30 x 14.5
I-2	Merino Wool/PA (70/30%) spun yarns, 36.0 x 2 + PET spun yarns with bio-ceramic additives Mirawave® 29.4 Enamelled copper wire, 0.07 mm (length 10 m, distance between wires in the fabric 0.65 cm)	E1, E3, E4, E5, E6, E7, E8, E9, E11, E12, E13, E14, E15, E16 E2, E10	30 x 19.5
I-3	Merino Wool/PA (70/30%) spun yarns, 36.0 x 2 + PET spun yarns with bio-ceramic additives Mirawave® 29.4 Enamelled copper wire, 0.07 mm (length 8.5 m, distance between wires in the fabric 0.65 cm)	E1, E3, E4, E5, E6, E7, E8, E9, E11, E12, E13, E14, E15, E16 E2, E10	30 x 16.5

Table 2. Description of different conductive weft knitted fabrics used for heating element II. Note: Number of stitches per unit length and unit area, cm^{-1} : Courses, P_V – 13, Wales, P_H – 8; Mass per unit area, g/m^2 – 370 ± 15.

Separate layers	Type of yarn, linear density, tex	Arrangement of yarns in pattern courses (knitting feeds) (Figure 3)		
		Element II-1	Element II-2	Element II-3
I-outer	PET spun yarns with bio-ceramic additives Mirawave®, 29.4	E1, E4	E1, E4, E7, E10	E1, E4, E7, E10, E13, E16, E19, E22
II-middle	PET spun yarns with bio-ceramic additives Mirawave®, 29.4	E2, E5	E2, E5, E8, E11	E2, E5, E8, E11, E14, E17, E20, E23
III-inner	PET/Silver twisted filament yarns Shieldex® [PET 11.3(f32) + PET silver coated 4.4 (f12)], 17,0 x 4 ply	E3	E3, E6	E3, E6, E9, E12
	PET spun yarns with bio-ceramic additives Mirawave®, 29.4	E6	E9, E12	E15, E18, E21, E24

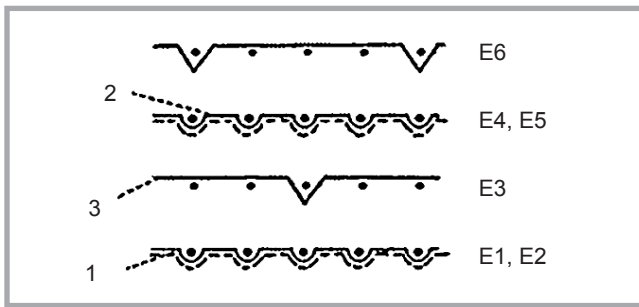


Figure 3. Pattern of the three-thread fleecy knitted fabric used for heating element II: 1 – plating yarn (outer layer), 2 – binding yarn (middle layer), 3 – fleece yarn (inner layer).

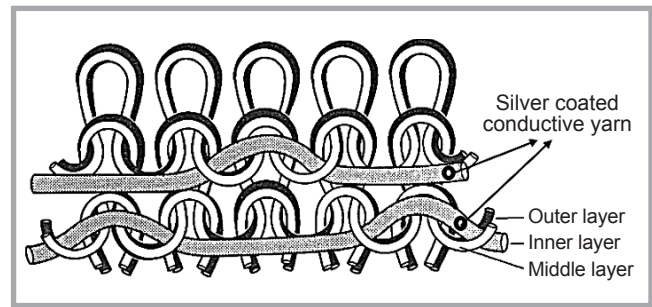


Figure 4. Structural view of the three-thread fleecy knitted fabric sample used for heating element II.

structure is shown in **Figure 3** and **Figure 4**. The number of stitches was calculated according to the LST EN 14971 [20] standard, and the mass per unit area was determined according to the LST EN 12127 standard [21].

Each loop creates a stage of the electrical circuit, with a definite resistance of each loop element. The head and legs of the loop of the yarn intersection can be considered as resistance points of the electrical circuit contacts and the intervals between them – resistors.

As shown in **Figure 4**, Shieldex® conductive yarns were integrated into the knitted structure on the inner side of the fabric (next to the skin) as a tuck loop-loop float.

Shieldex® is conductive yarn (twist factor $Z\ 300\ m^{-1}$) consisting of two twisted components: polyester 11.3 tex (f32) and polyester silver coated 4.4 tex (f12), developed by STATEX, Germany. 4-ply Shieldex® yarns (twist factor $S\ 100\ m^{-1}$) were used in the knitting process. The fleece yarns were manufactured using a PL 31C ring twisting machine.

The conductive yarns were situated as parallel elements in the knitted fabric. In order to obtain a heating circuit, the separate elements/tuck loop-loop float loop rows were connected to the parallel circuit by adding a textile based conductive chain on both of the shorter sides of the heating element. The chain was made of 30-ply silver coated polyamide (PA/Ag) $45.0 \pm 10\ tex$ (basic yarn count – 23.5 tex, f32, thickness of silver layer $\sim 1\ \mu m$) ELITEX® yarns. The quantity of plies was selected by performing experiments and choosing the most optimal connectivity and conductivity of the conductive textile chain.

Samples of heating elements were made with a heating area (length x height) – $(30 \times 16)\ cm^2$, selected as optimal to fit the majority of body sizes.

Water-repellent finishing was applied to the heating element to increase protection from the effect of care and wearing conditions. Fluorocarbon dispersion based on C-6, known as a water repellent agent, was applied on the knitted sample by a sprayer at room temperature. The drying – thermosetting process

was carried out in a laboratory oven and steamer machine at $100\text{--}140\ ^\circ C$, time – 7 min. The resistance of the sample to surface wetting (grade = 6) was measured according to the LST EN 24920:1997 standard [22].

In order to make the heating element resistant to care and wearing conditions and have permanent electric conductivity, a three-layer laminate was formed using a laboratory dry hot fusing machine. Layers were combined with thermoplastic $8\ g/m^2$ adhesive PA copolymer fabric.

Analyses of the heating effectiveness of the heating elements developed were performed using 4-wire (Kelvin method) method with direct current (DC). By changing the size of the current, the voltage and resistance were measured and the dependency on the heating element temperature analysed. Determination of the temperature values achieved was monitored by infrared images, taken with a thermal imaging camera – InfraredCam EU (FLIR® Systems) (see **Figure 5**). EM wave spectral range – $7.5 \div 15\ \mu m$, emissivity coefficient – 0.95. Textile materials exhibit a high emissivity coefficient ($0.92 \div 0.98$) [23]. The 4-wire method tests were performed according to the LST EN 16812:2014 standard [24].

An intelligent heating product with heating element II was tested in a field test on a real human at an ambient temperature of $19\ ^\circ C$ and additionally wearing a jacket on top. The microcontroller, which has a heating dynamics data storage function, was programmed to control the operations of the two heating elements. It was produced by means of 3D printing technologies. A model of the intelligent apparel product with two heating elements ensuring a comfortable microclimate for the user was

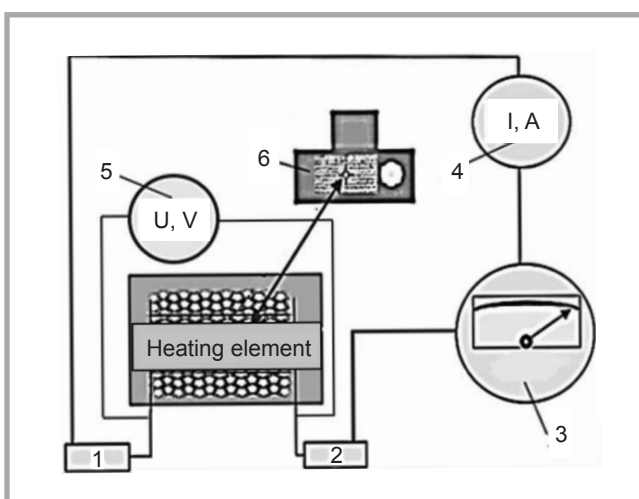


Figure 5. Experimental set-up for testing the heating behaviour of the knitted heating elements, where: 1, 2 – clamps, 3 – Keithley 2200 power source, 4 – UNI-T UT33C digital multimeter, 5 – UNI-T DT-890C digital multimeter, 6 – INFRA CAM thermal imaging camera (EM wave spectral range $7.5 \div 13\ \mu m$, emissivity coefficient – 0.95).

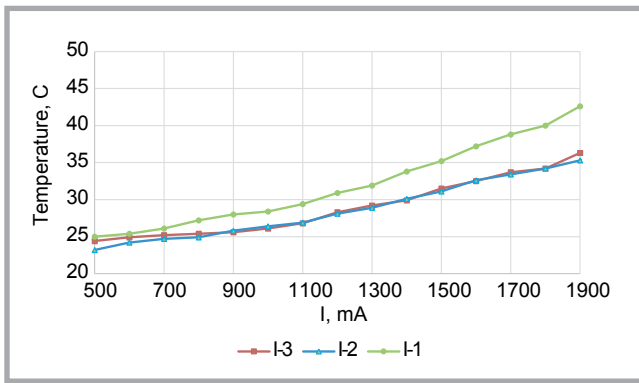


Figure 6. Dependence of the temperature of heating elements I-1, I-2 & I-3 on the current.

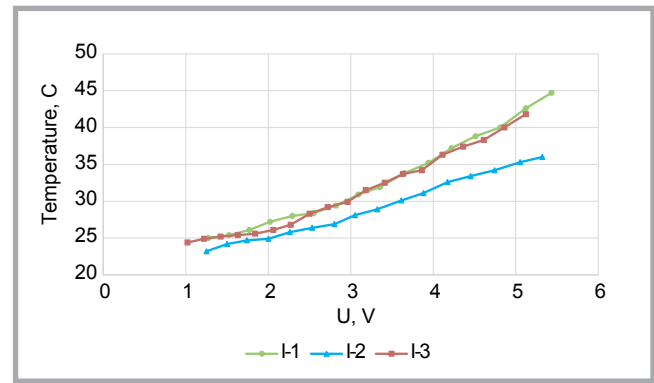


Figure 7. Dependence of the temperature of heating elements I-1, I-2 & I-3 on the voltage.

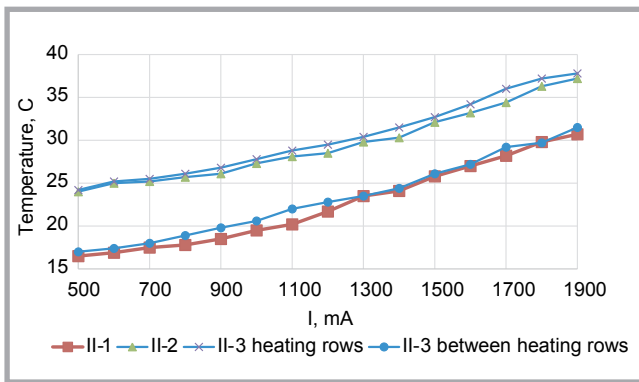


Figure 8. Dependence of the temperature of heating elements II-1, II-2, II-3 on current.

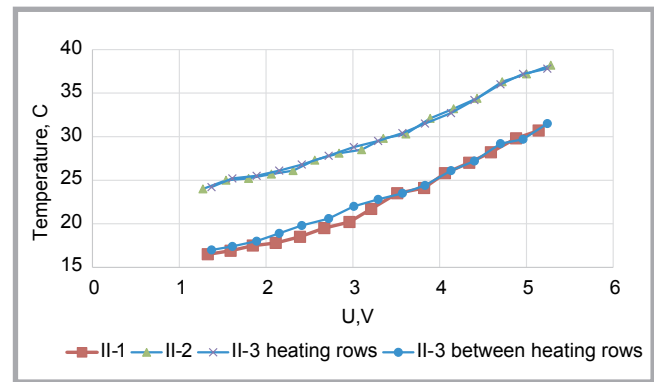


Figure 9. Dependence of the temperature of heating elements II-1, II-2, II-3 (heating rows) and II-3 (between heating rows) on the voltage.

created. Tests were performed by setting the maximum heating temperature allowed (39 °C) and a lower temperature of – 38 °C for both contours. Field tests were performed for the model created by wearing the product and setting the temperatures of both heating elements, from which the continuous operating time was determined.

The bending (flexural) rigidity B_{FAST} of the knits was determined according to the FAST (Fabric Assurance by Simple Testing) bending stiffness detection method [25, 26]. Knitted samples of 150 x 50 mm were tested in the longitudinal and crosswise directions. The bending rigidity B_{FAST} is calculated by the following formula:

$$B_{FAST} = W \times c^3 \times 9.807 \times 10^{-6}, \mu\text{N}\cdot\text{m}, \quad (1)$$

where, W – mass per unit area of specimen, g/m^2 ; c – bending length – half length ($l/2$) of bended specimen, mm;

Every measurement was performed 5 times for each experimental point, and the experimental results were statistically evaluated. The results are reliable as the variation of the values does not exceed 4.2%.

Results and discussion

The flexible heating elements developed for investigation vary in structure and electrical properties. In the first part of our research, we studied the effect of the current and voltage on the temperature of the heating elements. The results of two different heating elements and six different structures in total were investigated and presented in this research. Here, we attempted to show the dependence of the temperature of heating elements I-1, I-2, I-3, II-1, II-2 and II-3 on the current (see **Figure 6** and **Figure 8**) and voltage (see **Figure 7** and **Figure 9**).

The analysis showed (see **Figure 6**) that heating element I-1 with 10 metres of enamelled copper wire and with a 0.5 cm distance between wires in the fabric was the most effective and produced more heat at the same current rate. It means that a higher temperature or longer battery life is achieved while using heating element I-1 than for I-2 or I-3.

It was determined that heating element I-1 can generate more heat than I-2 and I-3 when applying the same current and voltage, i.e. a 6.2 °C higher temperature

at 1900 mA, and 0.5 °C higher at 5V. This can be due to the different length of the enamelled copper wire used in all three heating elements. The resistivity is higher when the length of the copper wire in the element is longer.

The study demonstrated that heating element I-2 had a similar temperature increase to element I-3 when varying the voltage. In any case, I-2 shows slightly better results and needs less power to reach the same temperature of the heating element.

From both results of the dependences of the temperature of heating element I on the current and voltage, we can state that heating element I-1 is the most effective from all three variants of heating element I.

The overall measurement results of heating element II are summarised in **Figure 8** and **Figure 9**. The highest temperature at the same current rate is achieved by heating element II-3; but the only disadvantage of such a result is that this temperature was measured when pointing to the heated row (stripe), while the temperature between the heating rows

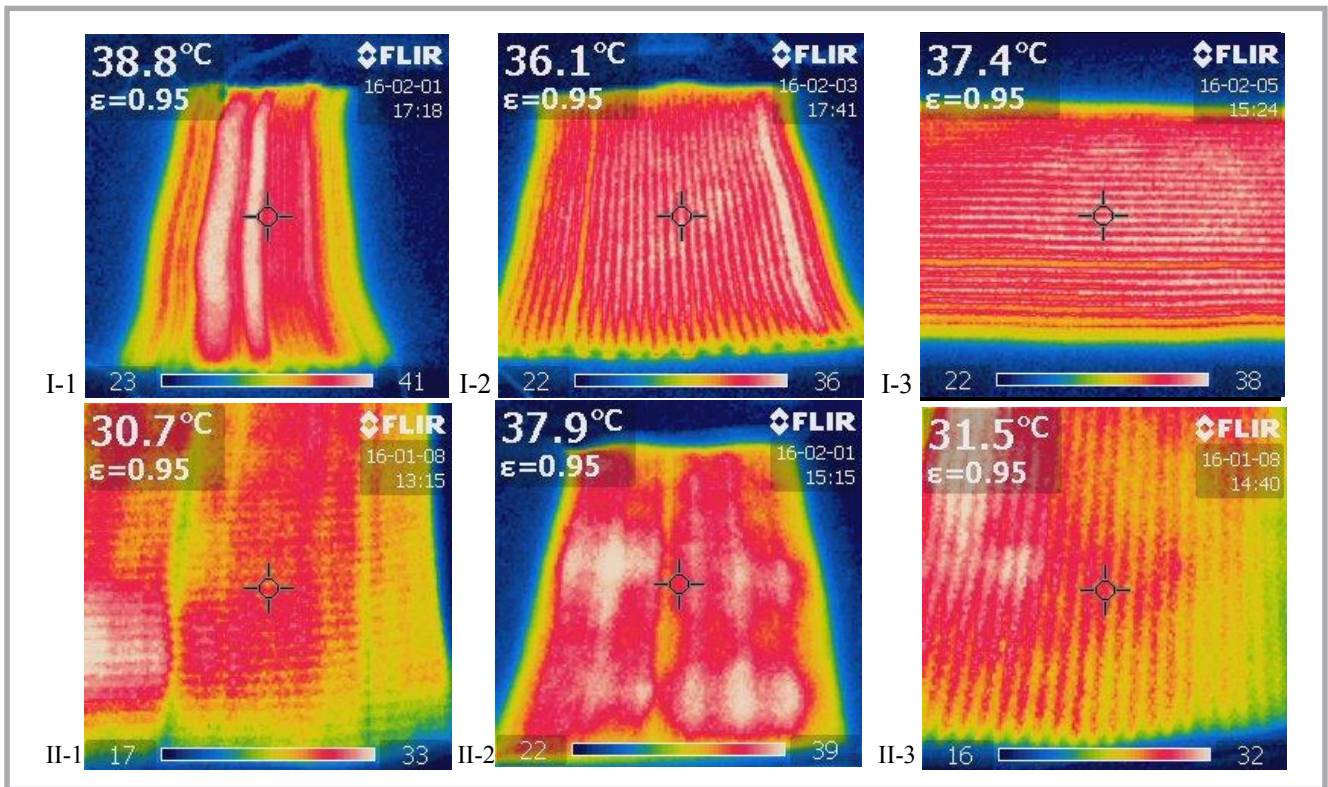


Figure 10. Results of investigation of the thermal signature of heating elements. The point of seeming temperature measurement is ringed.

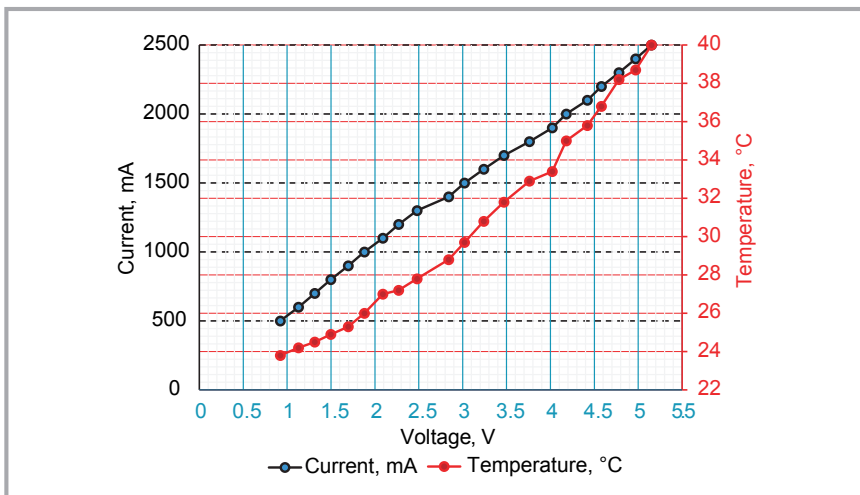


Figure 11. Temperature and voltage dependence on current, heating element II-2.

is significantly lower (see Figure 8). Heating element II-3 cannot demonstrate an equal heating area (see Figure 10). The thermal signature demonstrates visual heated rows, therefore the wearer is going to feel discomfort. To overcome this problem, it is necessary to choose heating element II-2 for further investigations, as the difference in temperature between II-2 and II-3 (heating rows) was not so significant, and the results of investigation of the thermal signatures of the heating elements showed that the heating area is even, with the heat well distributed. We achieved the same kind of tendencies for the dependence of the temperature of heating element II on the voltage as that on the current. The most

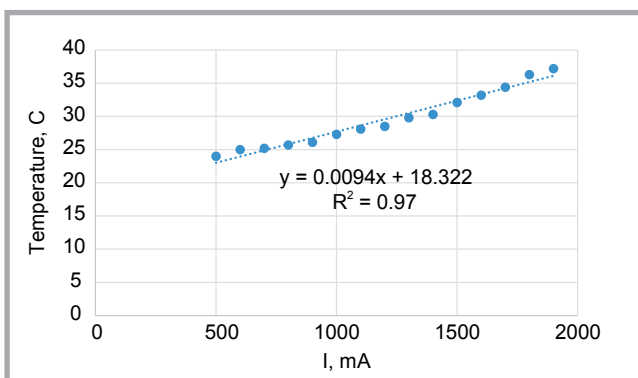


Figure 12. Dependence of temperature of heating element II-2 on the current.

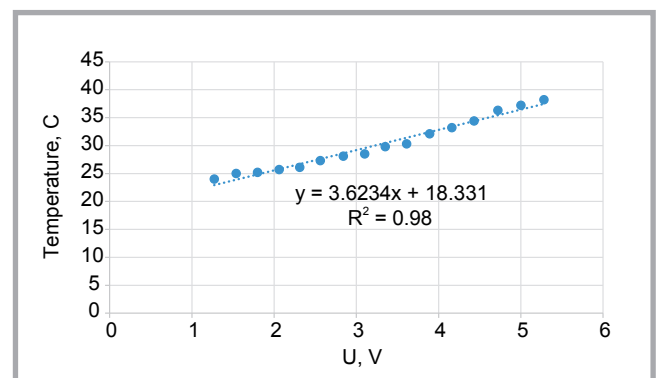


Figure 13. Dependence of the temperature of heating element II-2 on the voltage.

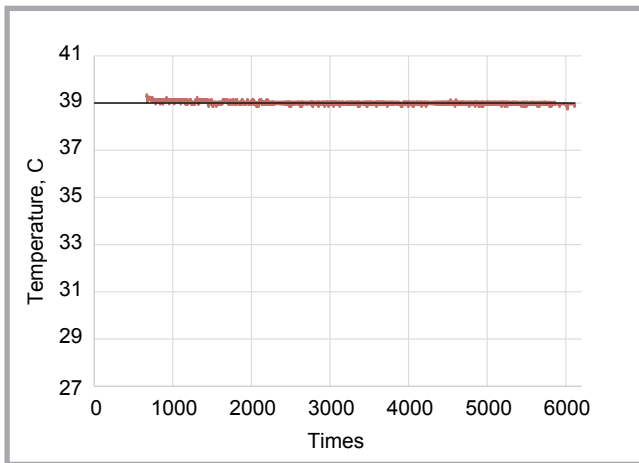


Figure 14. Upper contour temperature change by the microcontroller after setting a heating temperature of 39 °C.

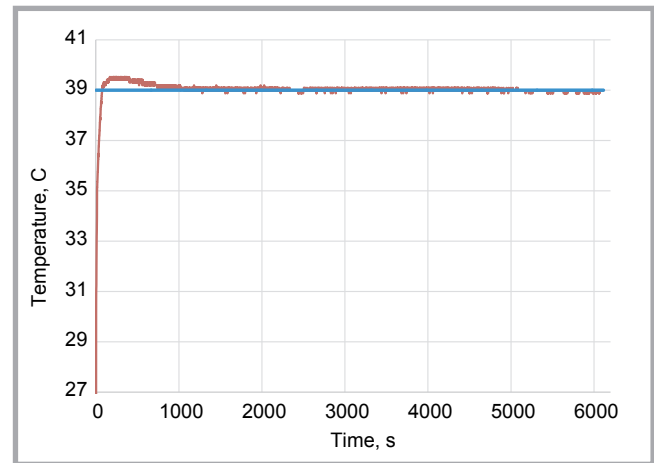


Figure 15. Lower contour temperature change by the microcontroller after setting a heating temperature of 39 °C.

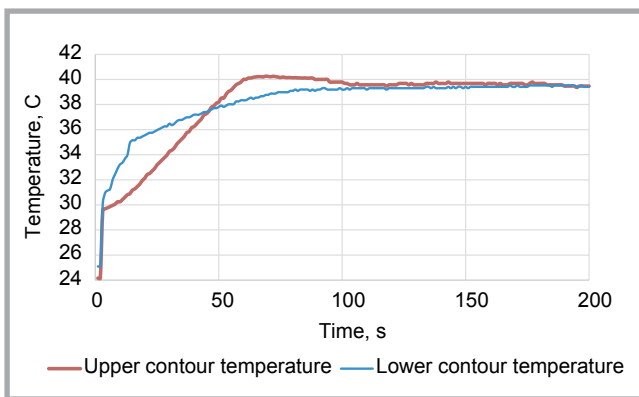


Figure 16. Fluctuation of the upper and lower contours in the first minutes with the heating temperature set to 39 °C.

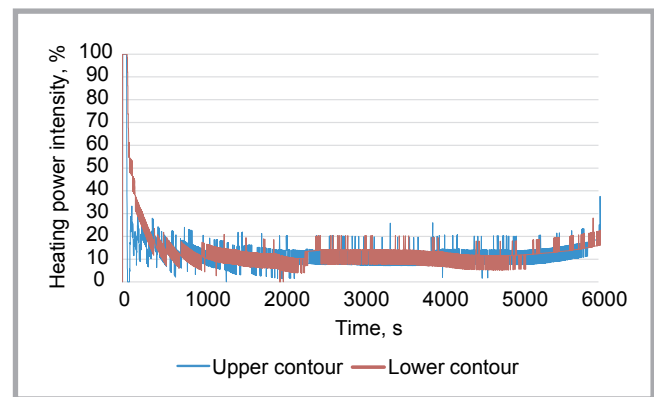


Figure 17. Heating power intensity of upper and lower contours when the microcontroller was set at a heating temperature of 39 °C.

effective was shown to be II-3 heating rows; but almost identical results were measured for element II-2. Keeping in mind the same uneven heating area of II-3, we decided to concentrate only on heating element II-2 (see *Figure 11*) in future investigations.

Results of the temperature of heating element II-2 for the different current and voltage applied are presented in *Figure 12* and *Figure 13*, respectively. The linear regression equations and coefficient of determination between the current or voltage and the temperature of heating element II-2 determined by the results of the tests are presented as well. As expected, the dependences are positive and a gradual change in temperature is observed. The influence of the current or voltage and temperature of heating element II-2 is significant, and the coefficient of determination ranges from 0.97 to 0.98. The linear regression equations obtained help to predict the change in temperature of the heating element when changing the current or voltage.

The bending rigidity of the heating elements investigated are presented in *Table 3*.

In the actual wear/field test, the intensity of the two contours was studied during the full exposure time. It was analysed when the intensity was highest and for how constant it was at the set temperature of the contours. It was also analysed how quickly the contour rises to the set temperature, as the temperature of the outline changes during the entire wear. All measurement data were recorded on the controller memory card and later used for analyses.

Table 3. Bending rigidity of knitted fabrics used for modelling of the heating elements investigated.

Code of heating element	B_{FAST} , 10^{-6} Nm	
	Longitudinal direction	Crosswise direction
I-1	35.31	734.24
I-2, I-3	34.52	539.39
II-1	14.86	12.25
II-2	16.30	13.51
II-3	17.83	14.86

The actual field test was performed using the upper and lower contours. Test results after setting the maximum allowable temperature of 39 °C for both contours are presented in *Figure 14* and *Figure 15*. The upper and lower contours were operating at the maximum set point, with an external battery of 3300 mAh, for 1 hour 41 min (6113 s). *Figure 14* and *Figure 15* provide graphic images of the warm-up time for both heating circuits

The temperature of both heating contours rose to the set maximum temperature of 39 °C in under two minutes and ensured

a constant temperature of contours and body skin for the rest of the period (**Figure 16**).

Graphs of the heating power intensity of the upper and lower contours, which are regulated by the device using the principle of pulsed modulation, are presented in **Figure 17**.

It is visible that the layout contours reach the set temperature. Initially the heating power intensity is 100%, i.e. when the heating circuit works at full capacity. When the temperature reaches 39 °C and stabilises, the heating circuit's power is limited, resulting in a significant reduction in the heating power and a further variation of 8 to 25%.

A lower temperature set on the microcontroller prolongs the heating time. When upper and lower contours were operating at a 38 °C set point with an external battery of 3300 mAh, the upper and lower contours were heated for 5 hours. A one degree Celsius difference in the settings means a 3 times longer working time of the battery.

Conclusions

Heating element I, made of wires, is not sufficiently flexible to be effectively applied in clothing or other wearable electronics. However, the conductive yarns used in heating element II provide necessary flexibility and stability, ensuring wearing comfort.

During this research, it was found that heating element II with silver coated yarns gave out warmth more evenly over all the resistive area. This was not achieved by heating element I, in which the areas where enamelled cooper wire was inserted were heated more than areas between wires.

The experiment's results also show that there is no significant difference in temperature between the centre and edges of heating element II.

As a result of this research, heating element II, which is made of 100% textile materials, is more suitable for the manufacture of a resistive heating element. The elements heat up at a voltage of 5 V to a temperature of 37.2 °C in less than two minutes. It is possible to raise the temperature until 39 °C, which is sufficient to ensure comfortable warmth for the user.

To show the trends of the temperature, linear regression equations were proposed. The coefficient of determination between the current or voltage and the temperature of heating element II-2 varies in the range of 0.97-0.98.

Field tests of the heating elements demonstrated that the set temperature is reached in less than two minutes, and that at the beginning the heating power intensity reaches 100%; but after the heating element achieves the set temperature, the heating power intensity drops, varying from 0 to 12%.

Acknowledgements

This research was supported by a grant (No. TEC-04/2015) from the Research Council of Lithuania.

References

1. Droval G, Glouannec P, Feller JF, Salagnac P. Simulation of Electrical and Thermal Behavior of Conductive Polymer Composites Heating Elements. *J. Thermophys. Heat Transf.* 19, 2005; 375-381.
2. El-Tantawy F, Kamada K, Ohnabe H. In Situ Network Structure, Electrical and Thermal Properties of Conductive Epoxy Resin–Carbon Black Composites for Electrical Heater Applications. *Mater. Lett.* 56, 2002; 112-126.
3. Sezgin H, Kursun Bahadır S, Boke Y E, Kalaoğlu F. Investigation of Heating Behaviour of E-textile Structures. World Academy of Science, Engineering and Technology. *International Journal of Environmental, Chemical, Ecological, Geological and Geophysical Engineering* 2015; 9: 482-485.
4. Stoppa M, Chiolerio A. Wearable Electronics and Smart Textiles: A Critical Review. *Sensors* 2014; 14: 11957-11992.
5. Hao L, Yi Z, Li C, Li X, Yuxiu W, Yan G. Development and Characterization of Flexible Heating Fabric Based on Conductive Filaments. *Measurement* 2012; 45: 1855-1865.
6. Nakad Z, Jones M, Martin T, Shenoy R. Using Electronic Textiles to Implement an Acoustic Beamforming Array: A Case Study. *Pervasive Mob. Comput.* 2007; 3: 581-606.
7. Roh Jung-Sim, Kim Sareum. All-fabric Intelligent Temperature Regulation System for Smart Clothing Applications. *Journal of Intelligent Material Systems and Structures* 2015; 1-11.
8. Šahta I, Baltina I, Truskovska N, Blums J, Deksnis E. Selection of Conductive Yarns for Knitting an Electrical Heating Element. *WIT Transactions on The Built Environment* 2014; 137: 91-102.
9. Cho G. Smart Clothing: Technology and Applications; CRC Press: Boca Raton, FL, USA, 2010; 30: 89-113.

10. Ghosh TK, Dhawan A, Muth JF. Formation of Electrical Circuits in Textile Structures. *Intell. Text. Cloth.* 2006; 239-282.
11. Parkova I, Vališevskis A, Kašurins A, Vīļumsone A. Integration of Flexible Key-pad into Clothing. *Proceedings of 8th International Scientific and Practical Conference "Environment Technology Resources"*, Rezekne, Latvia, June 2011; 20-22.
12. Schwarz A, Van Langenhove L, Guermontprez P, Deguillemont D. A Roadmap on Smart Textiles. *Text. Prog.* 2010; 42: 99-180.
13. Mather RR. Intelligent Textiles. *Rev. Prog. Color. Relat. Top.* 2001; 31: 36-41.
14. Wagner S, Bonderover E, Jordan WB, Sturm JC. Electortextiles: Concepts and Challenges. *Int. J. High Speed Electron. Syst.* 2002; 12: 391-399.
15. Randeniya LK, Bendavid A, Martin PJ, Tran C-D. Composite Yarns of Multiwalled Carbon Nanotubes with Metallic Electrical Conductivity. *Small* 2010; 6: 1806-1811.
16. Cristian I, Nauman S, Cochrane C, Koncar V. Electro-conductive Sensors and Heating Elements Based on Conductive Polymer Composites in Woven Fabric Structures. *Advances in Modern Woven Fabric Technology*. Ed. Vassiliadis, S. Intech: Shanghai, China 2011; 1-22.
17. Hao Liu, Jin Li et al. Thermal-electronic Behaviours Investigation of Knitted Heating Fabrics Based on Silver Plating Compound Yarns. *Textile Research Journal* 2016; 86(13): 1318-1412.
18. Syed Talha Ali Hamdani, Anura Fernando, Muhammad Dawood Hussain, Prasad Potluri. Study of Electro-Thermal Properties of Pyrrole Polymerized Knitted Fabrics. *Journal of Industrial Textile* 2016; 46(3): 771-786.
19. Pahalagedara LR, Siriwardane IW, Tissera ND, Wijesena RN, Nalin de Silva KM. Carbon Black Functionalized Stretchable Conductive Fabrics for Wearable Heating Applications. *RSC Advances* 2017; 31: 18821–19416.
20. LST EN 14971. Textiles – Knitted Fabrics – Determination of Number of Stitches per Unit Length and Unit Area.
21. LST EN 12127. Textiles – Fabrics – Determination of Mass per Unit Area Using Small Samples.
22. LST EN 24920. Textiles fabrics – Determination of resistance to surface wetting (spray test)
23. Oahman C. Emittance Measurements Using AGEMA E-Box. Technical report, AGEMA, 1999.
24. LST EN 16812. Textiles and Textile Products – Electrically Conductive Textiles – Determination of the Linear Electrical Resistance of Conductive Tracks.
25. BS3356. Method for Determination of Bending Length and Flexural Rigidity of Fabrics.
26. Ancutienė K, Strazdienė E, Nesterova A. The Relationship between Fabrics Bending Rigidity Parameters Defined by KES-F and FAST Equipment. *Materials Science* 2010; 16, 4: 346-352.

Received 25.03.2019 Reviewed 06.01.2020